

Scanning electron microscopy studies of failure surfaces of short glass fibre - rubber composites

V. M. MURTHY, A. K. BHOWMICK, S. K. DE

Rubber Technology Laboratory, Chemistry Department, Indian Institute of Technology, Kharagpur 721302, India

The failure surfaces of short-glass fibre reinforced rubber composites have been examined by scanning electron microscopy. The tensile, tear, flexing and abrasion modes have been studied. The different modes generate typical fracture surfaces depending on the nature of the test. The technical properties of the composites with and without reinforcing carbon-black filler have been explained on the basis of fracture modes. For comparison, mixes without fibre have also been studied.

1. Introduction

The reinforcement of an elastomer with short fibres blends the strength and stiffness of the fibre with the soft and tough elastic matrix. Recently, short-fibre reinforced elastomer composites have gained importance due to considerable processing advantages and improvement in certain mechanical properties. The performance and properties of these composites depend on variables such as fibre concentration, fibre dispersion, fibre-matrix adhesion, the type of fibre, fibre content, and fibre aspect ratio. Many workers [1-8] have studied the change in mechanical properties of these composites with variation in the above parameters, but the nature of failure has not been studied in detail. In this paper the fracture surfaces of glass-fibre reinforced natural rubber composites after different types of failure (such as tensile, tear, flexing and abrasion) have been studied by scanning electron microscopy (SEM). Attempts have been made to explain the technical properties of these composites on the basis of the results of the SEM studies. For comparison, mixes without fibre have also been studied. Earlier, similar studies of fracture surfaces of carbon-black filled rubbers and copper-filled polyvinyl chloride composites have been reported by workers of this laboratory [9-12].

2. Experimental procedure

The formulations of the mixes are reported in Table I. Glass fibres, as supplied by Pilkington Fibres Limited, Bombay, were chopped to 6 mm length. Mixing was done on a 15.2 by 53 cm open mixing mill with a nip gap of 0.406 mm. During mixing care was taken to ensure that the fibre orientation was the same in all the mixes, that is, in the grain direction. In order to promote adhesion between the fibres and the matrix, SRH (silica-Resorcinol-Hexa) system was added to the compound. Mixes were vulcanized at the respective optimum cure times. Preparation of vulcanizates was the same as described earlier [13]. Tensile and tear testing were done according to ASTM methods D412-51T and D624-54, respectively, and the samples were cut along the fibre direction. Flexing was carried out in a De Mattia flexing machine, according to ASTM D430-73 method at 70°C, and abrasion, in a Croydon-Akron machine using B.S. 903, Pt. 49:1957 method C.

For SEM studies the failure surfaces were sputter-coated with gold and the SEM photographs were taken with a Phillips model 500 within three days of testing. The orientation of the photographs was kept constant for a particular mode of testing for all samples.

TABLE I Formulations of mixes

Parameter	Content of mix (parts by weight)				
	A	B	C	D	E
Natural rubber*	100	100	100	100	100
Zinc oxide	5	5	5	5	5
Stearic acid	2	2	2	2	2
Resorcinol	2.5	0	2.5	2.5	2.5
HAF black (N 330)	0	40	40	0	40
Naphthenic oil	0	4	4	0	4
Vulcasil-S†	15	0	15	15	15
Glass fibre	0	0	0	25	25
CBS‡	0.8	0.8	0.8	0.8	0.8
Sulphur	2	2	2	2	2
Hexa§	1.6	0	1.6	1.6	1.6
Optimum cure time (in min) at 150° C	12.75	10.25	17.25	8.75	13.75

*Crumb rubber ISNR grade-5, as supplied by Rubber Research Institute of India.

†Reinforcing silica filler, supplied by Bayer India Ltd.

‡N-Cyclohexyl-2-Benzothiazyl Sulfenamide, supplied by Alkali and Chemical Corporation of India Ltd.

§Hexamethylene tetramine, supplied by E. Merck AG.

3. Results and discussion

3.1. The tensile fracture surface

Values of the tensile strength of Mixes A to E are given in Fig. 1a. Of the Mixes A to E, Mix B containing carbon black, silica and fibre shows the highest tensile strength. In general, addition of glass fibre lowers the tensile strength values. Micrographs for these are given in Figs 2a–c.

The silica filled mix (Mix A) ruptures with the formation of a network of silica aggregates (see Fig. 2a). These aggregates may be causing inhomogeneities and thus making the stress distribution non-uniform. The low strength of Mix A may be due to this factor. Addition of reinforcing carbon black (Mixes B and C) makes the fracture surface rough (Figs 2b and c). The layer delamination in the case of Mix C, shown in Fig. 2c, becomes prominent, leading to the sudden rupture of the specimen. For Mix D, without carbon black and with glass fibre, Fig. 2d shows the flow of material across the surface, with round holes left after pulling of the fibres and voids created by flow. Mix E with carbon black, silica and glass fibres indicates the same kind of fracture but the material flow is restricted (see Fig. 2e).

In the case of fibre reinforcement the matrix transmits the load mainly to the fibres whereas in the case of particle reinforced composites the matrix will carry the load and the reinforcing particles restrict the dislocation and slip of the matrix. It is also believed that in fibre reinforced composites the fracture occurs in two modes [14].

These are (a) breakage of fibre leading to failure and (b) pull-out of several fibres from the matrix. From the micrographs it is quite evident that the pull-out of fibres from the matrix is the main reason for the failure. The debonding of fibres may take place due to (a) insufficient fibres to restrain the matrix and thereby large strains develop on the matrix at low stresses or (b) weak fibre–matrix adhesion.

3.2. The tear fracture surface

The values of tear strength of Mixes A to E are given in Fig. 1b. Mix B shows the highest value for tear strength. The pair of mixes A and D and the pair C and E show almost the same values for tear strength, indicating that glass fibre does not affect the tear strength. The micrographs of the tear surfaces for these mixes are given in Figs 3a to d.

The fracture in the fibre reinforced composites with and without reinforcing carbon black is due to the failure of the fibre–matrix interface. There is no tear path on the fracture surface. Although the carbon-black filled matrix shows deformation through slip blocks or slip planes (see Fig. 3a), the silica-filled matrix shows a network of silica aggregates as in the case of tensile fracture. The formation of silica aggregates is evident even in Mix C. The fracture is nucleated from one such aggregate as shown in Fig. 3b. The material flow in case of Mix D, shown in Fig. 3c, is restricted with the addition of reinforcing black in Mix E (see Fig. 3d). It seems that the tearing energy is distributed

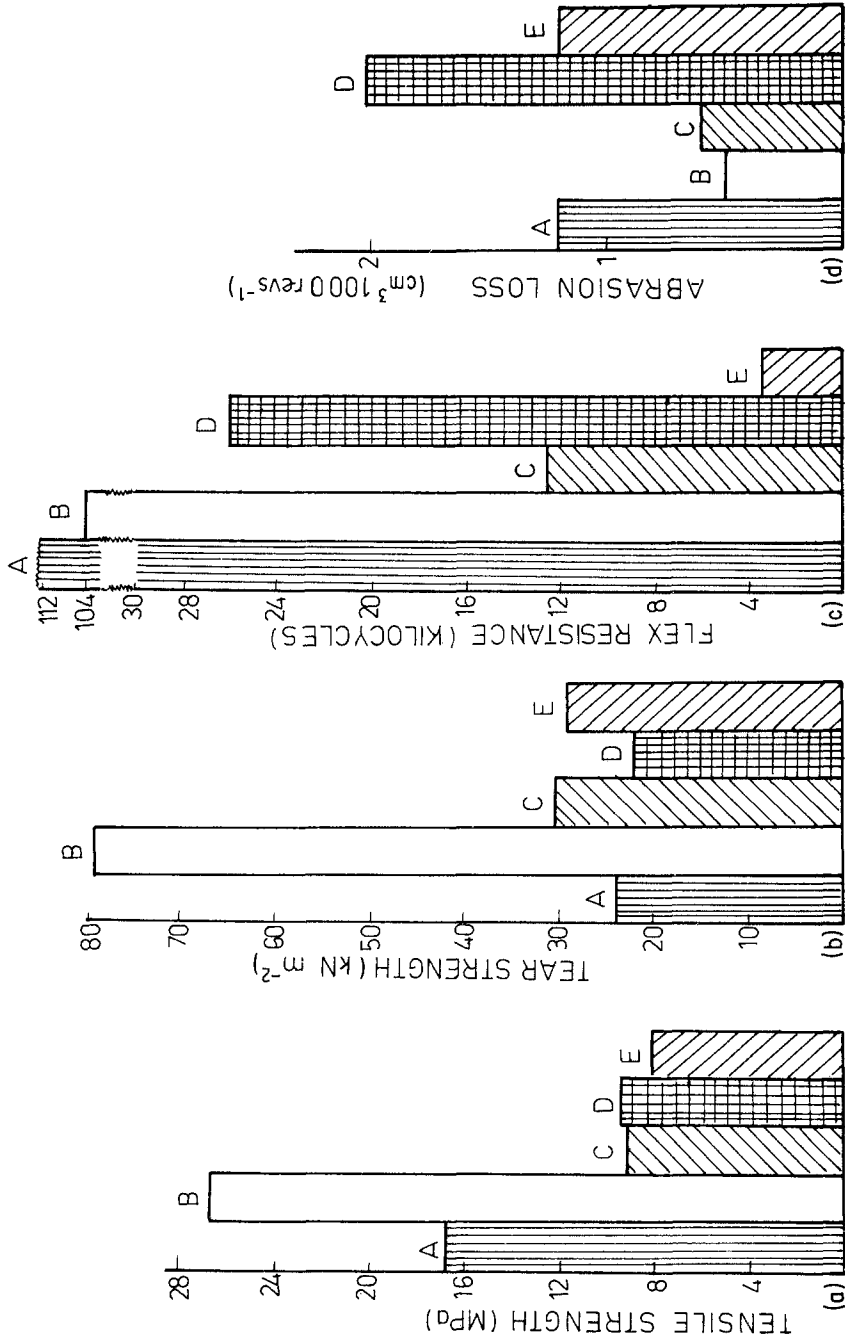


Figure 1 Histogram showing technical properties of the Mixes A to E, (a) tensile strength, (b) tear strength, (c) flex resistance and (d) loss by abrasion.

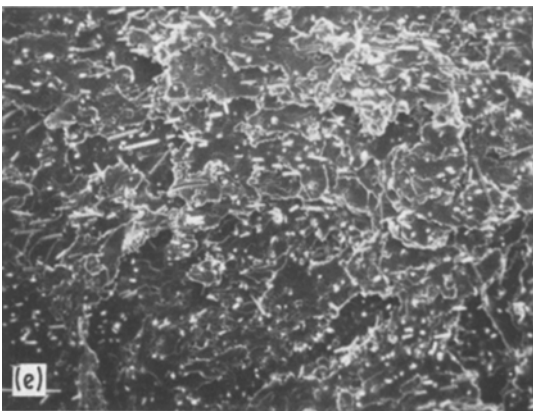
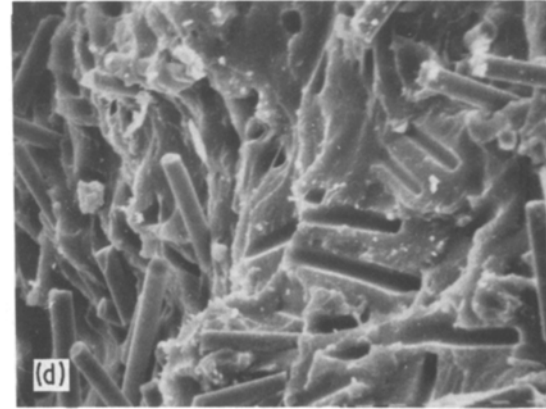
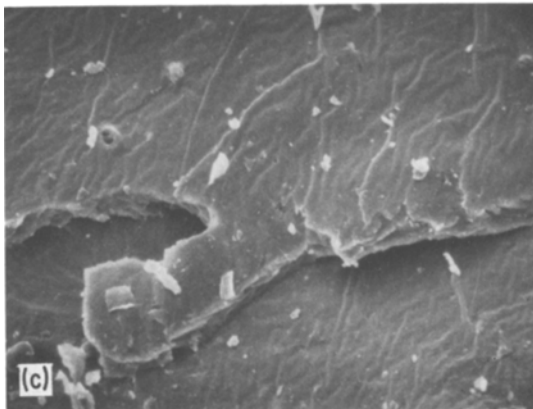
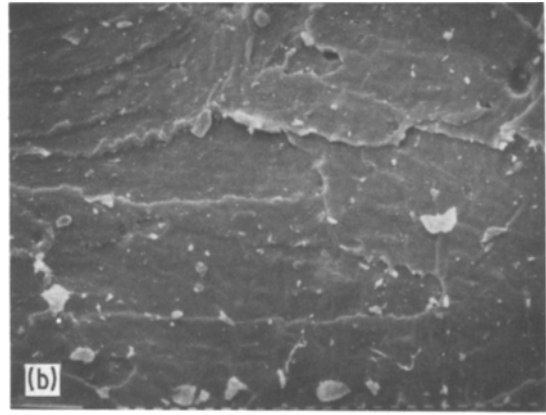
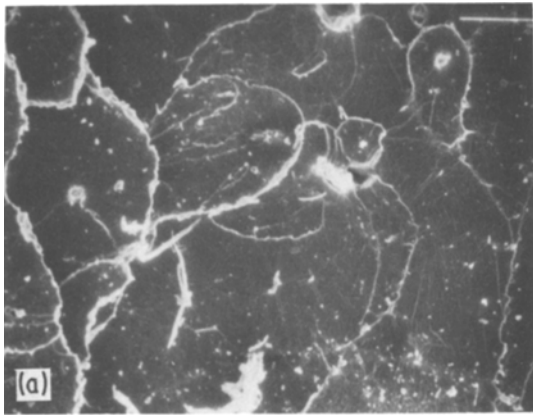


Figure 2 SEM photographs of tensile fracture surfaces, showing (a) network of silica aggregates (magnified 50 times) (b) rough surface of Mix B ($\times 50$) (c) layer delamination ($\times 200$) (d) fibre–matrix interface failure ($\times 400$) and (e) restricted material flow ($\times 50$).

through the matrix. There are fewer voids in Mix E as the material flow is restricted. Because of the restricted flow and fewer voids, the tear strength of Mix E is high. As for the case of tensile failure, the failure of the fibre–matrix interface leads to fracture.

3.3. The flexing fracture surface

The flex resistances of the Mixes A to E are given in Fig. 1c. Mix A shows the highest flex resist-

ance and Mix E shows the lowest resistance. Comparison of the two pairs (that is, Mixes A and D and Mixes C and E) shows that the addition of glass fibres lowers the flex resistance. It is also remarkable that the presence of carbon-black filler drastically reduces the flex resistance, as is evident for Mixes D and E. Micrographs for the flexing fracture surfaces of these mixes are given in Figs 4a to e.

Mix A, which contains only silica, shows a dimple structure and there are no cracks on the surface (see Fig. 4a). Mix A registers the maximum flex resistance. Mix B, shown in Fig. 4b, which contains only reinforcing carbon-black, shows elongated flows, rubber balling and a few cracks on the surface. Rubber balling has also been reported previously by De and co-workers [9] in the failure surfaces of flexed natural rubber vulcanizates. The

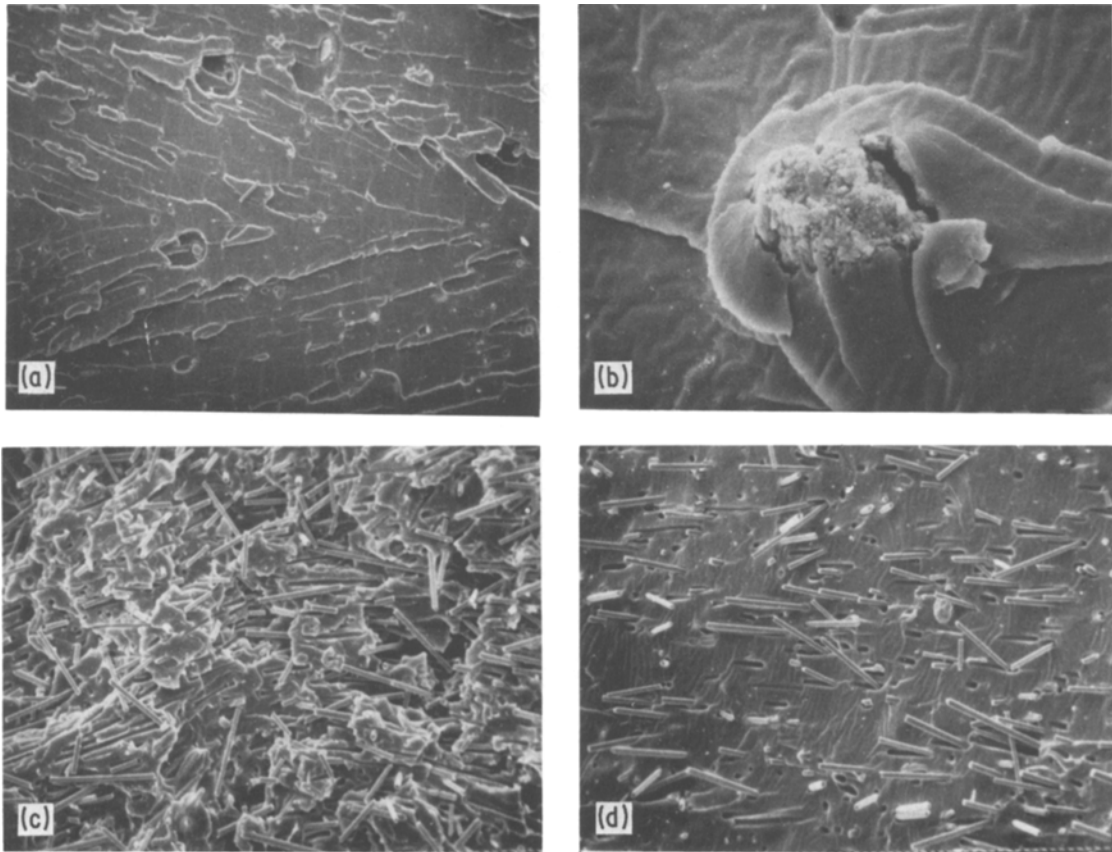


Figure 3 SEM photographs of tear fracture surfaces showing (a) ragged surface ($\times 50$) (b) silica aggregates ($\times 400$) (c) orientated fibres and voids ($\times 100$) (d) alignment of fibre ($\times 200$)

cracks increase in number in Mix C which contains carbon black and silica (see Fig. 4e). Rubber balling and the ductile nature of the matrix are also evident in Mix C as they are in Mix B. The lower flex resistance in these mixes may be ascribed to the large number of cracks on the surface. As soon as the fibre is introduced into the mix containing silica, Mix D, the nature of the failure is modified by an additional factor, namely, the failure of adhesion between the fibres and the matrix shown in Fig. 4d. The fracture surface also shows a large number of holes, broken fibres and a crumbled surface, but no crack is visible on the surface. Since the glass fibre has a higher modulus and hardness than the rubber matrix, the stress concentrates mostly on the fibre and the fibre–matrix interface is under dynamic test. Hence the failure occurs through the fibre–debonding and fibre–breakage. When carbon black is introduced (Mix E), the flex resistance further decreases. This is clearly evident from the large

and wavy cracks in Fig. 4e, in addition to round holes and broken fibres.

3.4. Abraded fracture surface

The results of abrasion loss for Mixes A to E are given in Fig. 1d. The abrasion loss of Mix B, containing carbon black, is minimum and that of Mix D is maximum. In general, addition of glass fibre increases the abrasion loss, as can be seen by comparing Mix A with Mix D and Mix C with Mix E, whereas the presence of carbon black reduces the abrasion loss, as exemplified by Mix A and Mix C, and Mix D and Mix E. The micrographs of the abraded surfaces are given in Fig. 5a to f.

Mix A, shown in Fig. 5a, shows ridges, and there are holes on the surface. The carbon-black filled compound (Mix B), shown in Fig. 5b, shows coarse ridges as observed earlier [9]. The fracture surface of Mix C, containing both carbon black and silica shows the material flow across the sur-

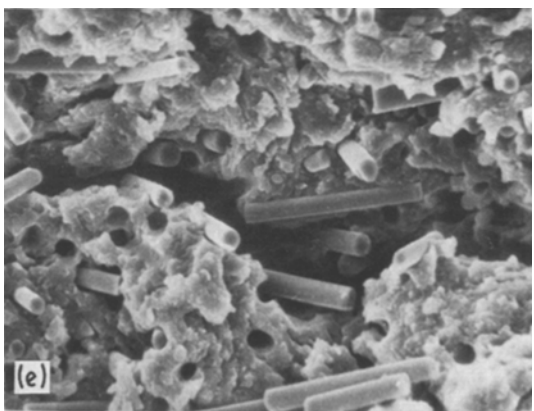
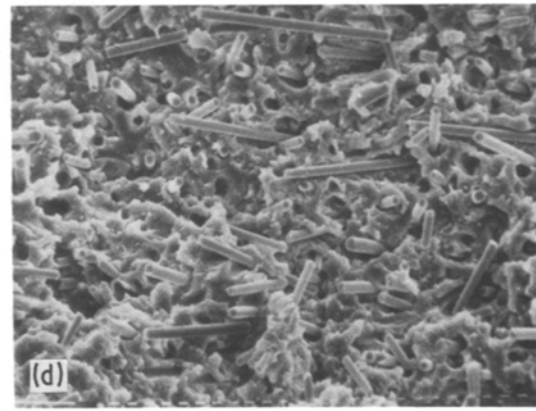
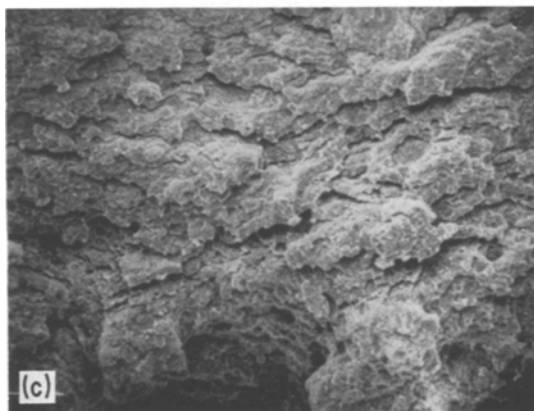
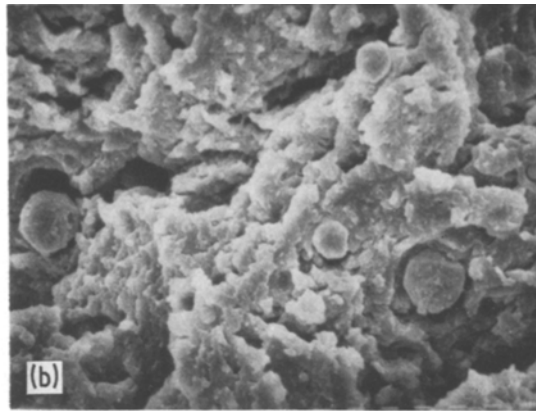
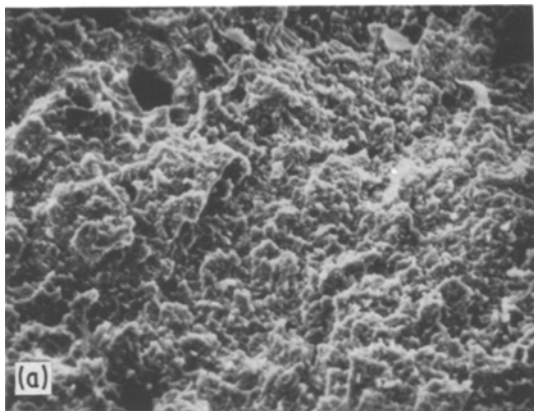


Figure 4 SEM photographs of flex fracture surfaces, showing (a) dimple structure on the surface ($\times 100$) (b) rubber balling ($\times 400$) (c) parallel cracks ($\times 50$) (d) fibre–matrix interface failure ($\times 200$) and (e) a continuous crack ($\times 400$).

face (see Fig. 5c) indicating the tendency to form ridges. The glass fibre reinforcement, either in non-filled or carbon-black filled compounds does not change the mechanism of abrasion. Fig. 5d shows the ridge on the abraded surface of Mix D. The structure of the rib shown in Fig. 5e shows debonded and broken glass fibres in the crumbled surface. The fracture surface of Mix E shows coarse, parallel and close ridges with cracks occurring beneath the ridges (see Fig. 5f).

On introduction of glass fibre into the matrix the same abrasion pattern is observed (see Fig. 5d) as in the case of carbon-black filled compounds and hence the loss is mainly due to the fatigue wear of the materials. The roll formation by the matrix on the surface indicates that the stress is distributed and worked throughout the surface. The weight loss is mainly due to loss of glass fibre either by interfacial failure or by fibre breakage. Since the amount of glass fibre per unit weight of the matrix is greater in Mix D than in Mix E, the weight loss is maximum for Mix D.

4. Conclusions

(a) The fracture surfaces of short glass-fibre reinforced natural rubber composites manifest typical characteristics depending on the nature

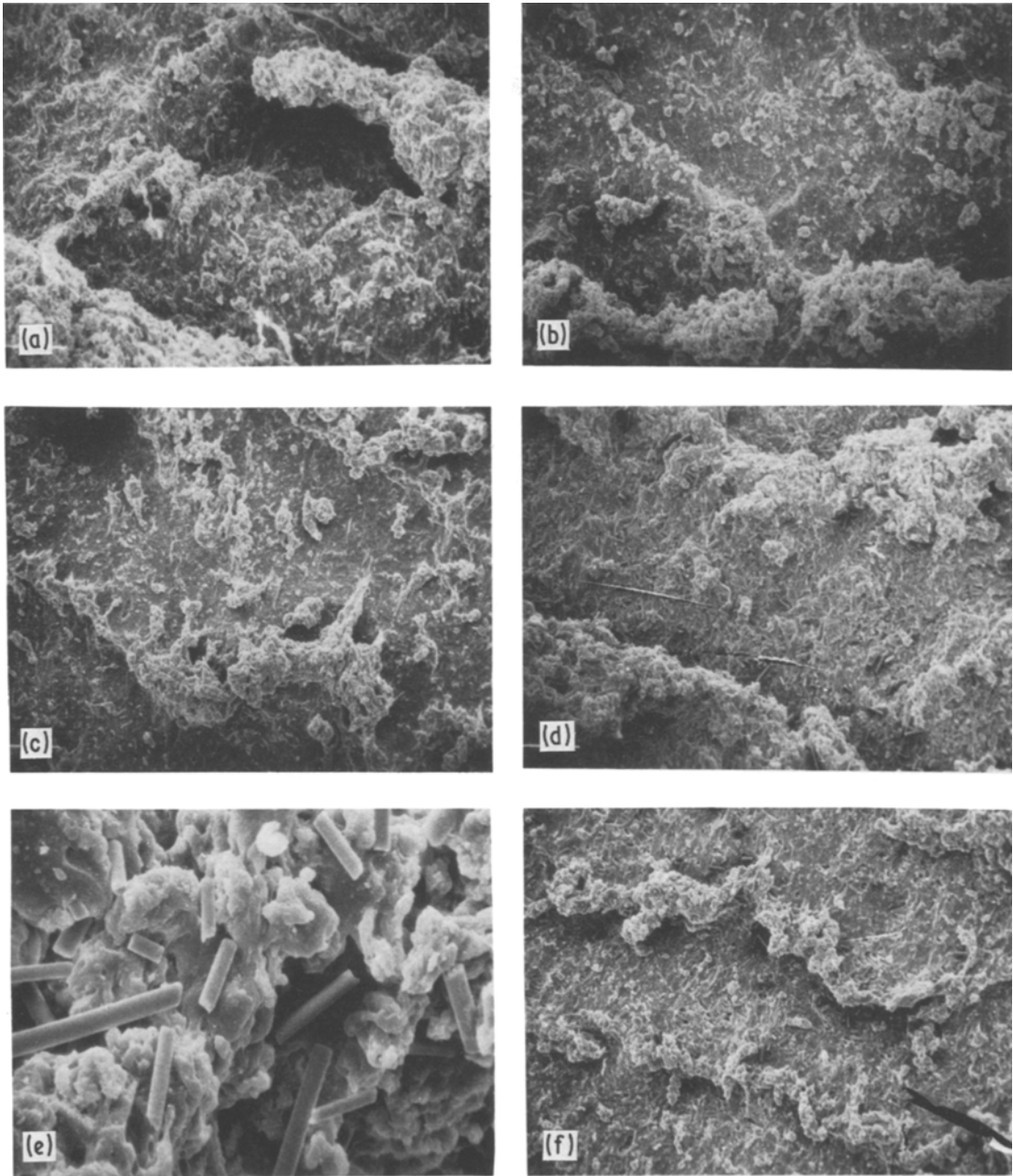


Figure 5 SEM photographs of abraded fracture surfaces, showing (a) ridges and holes ($\times 50$) (b) coarse ridges ($\times 50$) (c) material flow ($\times 50$) (d) ridges ($\times 50$) (e) structure of the rib with debonded fibres ($\times 400$) and (f) close ridges with cracks beneath ($\times 50$).

of the test. However, the mechanism of failure is mainly due to the fibre–matrix interface. Only in the case of abrasion, is fibre breakage prominent.

(b) The failure mechanism of composites with and without fibre is different in the case of tensile, tear and flexing fracture, but the abraded fracture surface shows ridges independent of fibre content.

Acknowledgement

The SEM studies were carried out at the Regional Sophisticated Instruments Centre, Bose Institute, Calcutta with the assistance of Dr T. Guha and Mr R. Bhar. The authors gratefully acknowledge financial support for this project from the Council of Scientific and Industrial Research, New Delhi.

References

1. B. E. BROKENBROW, D. SIMES and A. L. STOKOE, *Rubber J.* **151** (1969) 61.
2. G. C. DERRINGER, *J. Elastoplast.* **3** (1971) 230.
3. *Idem*, *Rubber World* **165** (1975) 45.
4. J. E. O'CONNOR, *Rubber Chem. Technol.* **50** (1977) 945.
5. A. Y. CORAN, *ibid.* **47** (1974) 396.
6. A. Y. CORAN, P. HAMEED and L. A. GOETTLER, *ibid.* **49** (1976) 1167.
7. A. Y. CORAN, K. BOUSTANY and P. HAMEED, *J. Appl. Polym. Sci.* **15** (1975) 2471.
8. B. K. I. KU ABD RAHMAN and C. HEPBURN, Proceedings of the International Conference on Structure-property relations of rubber, Kharagpur, India, December 1980.
9. A. K. BHOWMICK, G. B. NANDO, S. BASU and S. K. DE, *Rubber Chem. Technol.* **53** (1980) 327.
10. A. K. BHOWMICK, S. BASU and S. K. DE, *ibid.* **53** (1980) 321.
11. *Idem*, *J. Mater. Sci.* **16** (1981), 1654.
12. S. K. BHATTACHARYA, S. BASU and S. K. DE, *Polymer Eng. Sci.* **19** (1979) 540.
13. A. K. BHOWMICK and S. K. DE, *Rubber Chem. Technol.* **53** (1979) 985.
14. L. J. BROUTMAN and R. H. KROCK, "Modern Composite Materials", (Addison-Wesley Publishing Company, Massachusetts, 1967) p. 79.

*Received 30 April
and accepted 23 July 1981*